

CERN-TH.7308/94
Technion-PH-94/9
hep-ph/94mmnnn

On the Determination of $|V_{ub}|$ from Inclusive Semileptonic Decay Spectra

Boris Blok

Physics Department, Technion, Haifa, Israel

Thomas Mannel

Theory Division, CERN, CH-1211 Geneva 23, Switzerland

Abstract

We propose a model independent method to determine $|V_{ub}|$ from the energy spectrum of the charged lepton in inclusive semileptonic B decays. The method includes perturbative QCD corrections as well as nonperturbative ones.

CERN-TH.7308/94
June 1994

1 Introduction

Recently the inclusive decay spectra of heavy hadrons have attracted renewed attention. It has been shown that by a combination of Heavy Quark Effective Theory and the Operator Product Expansion one may perform a systematic $1/m_Q$ expansion of the charged lepton spectrum in inclusive heavy hadron decays [1] - [8]. However, it turns out that an adequate description of the endpoint region, where the charged lepton energy $E_\ell \sim E_{max}$, requires a partial resummation of the Operator Product Expansion, yielding a result analogous to the leading twist terms in deep inelastic scattering. In particular, it involves the analogue of the parton distribution function, which in the present case describes the endpoint region of the lepton spectrum. While in most of the phase space the nonperturbative corrections may be described in terms of a few parameters, the endpoint region needs the input of a nonperturbative function [9]-[11]. These recent ideas constitute a substantial conceptual progress towards a model independent description of inclusive decay spectra, including the endpoint region.

However, aside from the nonperturbative effects one also has to include QCD radiative corrections before one may confront the theory with data. These corrections have been calculated [12]-[16] and are known to be small for $b \rightarrow c$ transitions over the whole phase space. This is also true for the $b \rightarrow u$ case, as long as one is not too close to the endpoint $E_\ell \sim E_{max}$. Neglecting the mass of the u quark one finds Sudakov-like double logarithms of the form $\ln^2(E_{max} - E_\ell)$ as well as single logarithms $\ln(E_{max} - E_\ell)$, indicating a breakdown of perturbation theory close to the endpoint.

In the present context the QCD radiative corrections have been studied by Falk et al.[17] and Bigi et al.[10]. Falk et al. arrive at the conclusion that the endpoint region of the $b \rightarrow u$ decays is strongly affected by QCD radiative corrections and in principle a resummation to all orders becomes necessary. The conclusion of [17] is that the extraction of the nonperturbative effects becomes practically impossible due to large and mainly uncontrollable perturbative effects.

In [10] the Sudakov logarithms are exponentiated leading to a strong modification of the endpoint region. The authors of [10] suggest that uncontrollable radiative corrections discussed in [17] may be eliminated by the appropriate choice of the scale μ entering the strong coupling. They use $\mu \sim \Lambda m_b$, where Λ is the characteristic momentum of light degrees of freedom in the heavy meson. However, this leads to a strong modification of the shape of the spectrum near the endpoint and the reliability of the calculation becomes questionable.

Unfortunately, it is only the endpoint region of charmless B decays, which is not buried in the huge background of the charmed decays. The kinematic endpoint of the charmed B decays is $(m_B^2 - m_D^2)/(2m_B) \sim 2.3$ GeV, while for

the charmless semileptonic decay it is $(m_B^2 - m_\pi^2)/(2m_B) \sim 2.6$ GeV. Hence there is only a window of at maximum 300 MeV, which may be attributed solely to the transition $b \rightarrow u\ell\nu$. The size of this window is of the order of the mass difference of the heavy meson and the heavy quark, $\bar{\Lambda} = m_B - m_b$, and thus it is not dominated by a few resonances. This would be the case in a smaller region of the size $\bar{\Lambda}(\bar{\Lambda}/m_b)$, which is of the order of tens of MeV, and in which methods mentioned above would fail, since they are based on parton hadron duality.

The present paper is an attempt to define quantities which are on one hand experimentally accessible, and on the other hand allow to disentangle perturbative and nonperturbative effects. Our suggestion is to calculate appropriate moments \mathcal{M}_n of the measured spectrum, which are defined in such a way that they allow an expansion in both $\alpha_s(m_b)$ and $\bar{\Lambda}/m_b$, at least for some range of indices n .

Similar ideas have been put forward previously in [9] and [10]. However, in these papers there has been no detailed numerical study of such moments, including both radiative and nonperturbative effects.

In the next section we shall reconsider the perturbative and nonperturbative contributions to the decay spectrum of inclusive semileptonic charmless B decays and give the definition of the moments. In section 3 we perform a numerical study from which we obtain constraints on the range of the index n of the moments. Finally we give our conclusions and comment on the extraction of V_{ub} .

2 Perturbative and Nonperturbative Contributions to the Spectrum

It has been shown in [1] -[8] that one may obtain a systematic $1/m_b$ expansion for inclusive decay rates and the corresponding spectra. The leading term in this expansion is the free quark decay, and the first nonvanishing corrections appear formally at the order $1/m_b^2$. These are genuinely nonperturbative corrections, which are given in terms of two matrix elements

$$\langle B(v)|\bar{h}_v(iD)^2h_v|B(v)\rangle = 2m_B\lambda_1 \quad (1)$$

$$\langle B(v)|\bar{h}_v(-i)\sigma_{\mu\nu}(iD^\mu)(iD^\nu)h_v|B(v)\rangle = 6m_B\lambda_2. \quad (2)$$

The parameter λ_2 is given in terms of the $0^- - 1^-$ mass splitting $\lambda_2 = (m_{B^*}^2 - m_B^2)/4 \sim 0.12$ GeV 2 . The matrix element λ_1 is not as easily accessible, in particular it has not yet been determined experimentally. The theoretical estimates vary over a broad range [18, 19] of about $\lambda_1 \sim -(0.3 - 0.6)$ GeV 2 ; thus we shall consider below a typical “small” value $\lambda_1 = -0.3$ GeV 2 and a “large” one, $\lambda_1 = -0.6$ GeV 2 .

The result for the spectrum of the inclusive decay $B \rightarrow X_u \ell \nu$, neglecting the mass of the u quark, is given by

$$\frac{1}{\Gamma_b} \frac{d\Gamma}{dy} = \left[2y^2(3 - 2y) + \frac{10y^3}{3} \frac{\lambda_1}{m_b^2} + 2y^2(6 + 5y) \frac{\lambda_2}{m_b^2} \right] \Theta(1 - y) - \frac{\lambda_1 + 33\lambda_2}{3m_b^2} \delta(1 - y) - \frac{\lambda_1}{3m_b^2} \delta'(1 - y), \quad (3)$$

where

$$y = \frac{2E_\ell}{m_b} \quad \Gamma_b = \frac{G_F^2 |V_{ub}|^2}{192\pi^3} m_b^5. \quad (4)$$

The δ function singularities at the parton model endpoint $y = 1$ indicate a breakdown of the operator product expansion. In fact, it has been pointed out in [4, 5, 6] that for the decay spectra the expansion parameter is in fact $\bar{\Lambda}/[m_b(1 - y)]$, which becomes large close to the endpoint. Still these terms have an interpretation as being the first few terms of a moment expansion of a nonperturbative function describing the behavior of the spectrum close to the endpoint [9]-[11]:

$$\frac{d\Gamma}{dy} = \Gamma_b \left[2\Theta(1 - y) + \sum_{n=1}^{\infty} \frac{a_n}{m_Q^n} \frac{1}{n!} \delta^{(n-1)}(1 - y) \right] = 2\Gamma_b \int_{(y-1)m_b/\bar{\Lambda}}^1 F(x) dx, \quad (5)$$

where $\delta^{(k)}$ denotes the k th derivative of the δ function. Note that a_1 vanishes and a_2 may be read off from (3) to be $a_2 = -\lambda_1/3$.

The function $F(x)$ may be written formally as

$$F(x) = \frac{1}{2m_B} \langle B(v) | \bar{h}_v \delta \left(x - \frac{iD_+}{\bar{\Lambda}} \right) h_v | B(v) \rangle, \quad (6)$$

where D_+ is the positive light cone component of the covariant derivative. This function has support only in a region of $x \sim \mathcal{O}(1)$. In particular, the function F leads to some ‘‘smearing’’ of the endpoint region, with the effect that the endpoint of the spectrum is shifted from the parton model endpoint $m_b/2$ to the physical endpoint $m_B/2$, where m_B is the B -meson mass. Below we shall use some model input for F to estimate the size of the higher order corrections close to the endpoint.

Aside from these nonperturbative corrections there are also perturbative ones, which have been calculated some time ago. The order α_s corrections are known for all values of the lepton energy [12]-[16]; however, since we are interested only in the behavior close to the endpoint, we shall consider here only the contributions relevant in this region. It turns out, that the order α_s corrections exhibit doubly and singly logarithmic divergencies at the endpoint. Up to terms vanishing at the endpoint, the result reads [16]

$$\frac{d\Gamma}{dy} = \frac{d\Gamma^{(0)}}{dy} \left[1 - \frac{2\alpha_s}{3\pi} \left(\ln^2(1 - y) + \frac{31}{6} \ln(1 - y) + \frac{5}{4} + \pi^2 \right) \right], \quad (7)$$

where at the endpoint

$$\frac{1}{\Gamma_b} \frac{d\Gamma^{(0)}}{dy} = 2y^2(3 - 2y)\Theta(1 - y) \rightarrow 2\Theta(1 - y). \quad (8)$$

The scale μ of the strong coupling is not yet fixed in this expression; any scale choice will formally only affect subleading terms. However, from physical considerations one may be lead to chose $\mu \sim m_b^2(1 - y)$ as it was done in [10]¹, leading to an even more singular behavior as $y \rightarrow 1$. In any case, a resummation of the singular terms becomes mandatory in order to describe the spectrum close to the endpoint.

The common folklore is that the doubly logarithmic terms in (7) exponentiate, and at the level of the Sudakov logarithms the radiative corrections become

$$\frac{d\Gamma}{dy} = \frac{d\Gamma^{(0)}}{dy} \exp \left[-\frac{2\alpha_s}{3\pi} \ln^2(1 - y) \right]. \quad (9)$$

Again the problem arises of the scale of α_s and we shall compare below two choices. Using the one loop expression for α_s

$$\alpha_s(\mu) = \frac{12\pi}{(33 - 2n_f) \ln(\mu^2/\Lambda_{QCD}^2)}, \quad (10)$$

we will compare the results obtained for $\mu = m_b$ and $\mu \sim m_b^2(1 - y)$, the latter expression leading to

$$\frac{d\Gamma}{dy} = \frac{d\Gamma^{(0)}}{dy} \exp \left[-\frac{8}{25} \frac{\ln^2(1 - y)}{\ln[(m_b^2/\Lambda_{QCD}^2)(1 - y)]} \right]. \quad (11)$$

In the endpoint region one obtains qualitatively a behavior of the form [10]

$$\frac{d\Gamma}{dy} \sim \frac{d\Gamma^{(0)}}{dy} (1 - y)^{(\epsilon_0 - 1)}, \quad (12)$$

where

$$\epsilon_0 - 1 = -\frac{8}{25} \frac{\ln(1 - y)}{\ln[(m_b^2/\Lambda_{QCD}^2)(1 - y)]}$$

behaves approximately like a constant in the region of interest [10]. However, after such a resummation to all orders of perturbation theory, it is not obvious, how to disentangle perturbative and nonperturbative contributions any more. This becomes clear, if one really treats ϵ_0 as a constant, in which case one may rewrite (12)

$$\frac{d\Gamma}{dy} \sim \frac{d\Gamma^{(0)}}{dy} \text{const. } \exp \left\{ \frac{12\pi(\epsilon_0 - 1)}{25} \frac{1}{\alpha_s[(m_b^2/\Lambda_{QCD}^2)(1 - y)]} \right\}, \quad (13)$$

¹ Actually, the scale chosen in [10] is $\mu^2 \sim \bar{\Lambda}m_b$, but this is equivalent to $\mu \sim m_b^2(1 - y)$, since in the endpoint region $1 - y \sim \bar{\Lambda}/m_b$.

which in this form looks like a nonperturbative contribution.

The above discussion shows that the endpoint region is in fact difficult to describe. On one hand there are large nonperturbative contributions, on the other hand there are perturbative contributions, becoming large in the endpoint region. These remarks, however, apply only to the spectrum itself. It has already been shown in [9, 10] that it may be helpful to consider appropriately defined moments of the spectrum; e.g. the moments of the spectrum taken with respect to the parton model endpoint are related to the coefficients of the most singular δ function like singularities at the endpoint, in each order in the $1/m_b$ expansion.

Here we propose to consider a slightly different set of moments, namely

$$\mathcal{M}_n = \int_0^{1+\bar{\Lambda}/m_b} dy \, y^n \frac{d\Gamma}{dy}, \quad (14)$$

which may be rewritten in terms of the moments as defined in [9]. As we shall discuss in detail below, these moments have, for some range of n , a simultaneous expansion in $\alpha_s(m_b)$ and $\bar{\Lambda}/m_b$.

This range of n is specified by two requirements. Experimental information will be available only close in the endpoint region, and thus n has to be large enough to be sensitive to this region. On the other hand, the larger n is, the stronger the sensitivity to the details of the endpoint region is. In other words, only for not too large n one may perform the simultaneous perturbative and nonperturbative expansion; the problems present in the spectrum will reappear in the behavior of the moments \mathcal{M}_n for large n .

In fact, from order of magnitude considerations one would expect that there is no such range in n , where n is large enough to be sensitive to the endpoint, and in which nonperturbative and radiative effects still remain under control. However, it turns out from the more detailed study presented below that there might be such a window in n .

In the next section we shall perform a numerical study for the radiative corrections and the nonperturbative contributions, in order to find a range in n where one may reliably calculate the moments \mathcal{M}_n .

3 Numerical Discussion

We shall first consider the moments of the differential distribution in the naive parton model, without any corrections. The spectrum is given by the parton model expression and one obtains for the moments to the zeroth order

$$\mathcal{M}_n^{(0)} = \Gamma_b \frac{2(n+6)}{(n+3)(n+4)} \quad (15)$$

However, we are mainly interested in the endpoint region, where the parton model spectrum may be approximated by (8), and the moments obtained in this approximation are

$$\tilde{\mathcal{M}}_n^{(0)} = \Gamma_b \frac{2}{n+1} \quad (16)$$

In Fig.1 we plot the moments obtained from the full parton model rate versus the approximation (16). The comparison between the two sets gives some impression, at what n one is sensitive only to the endpoint region; from the figure one reads off that already at $n \sim 4$ one mainly obtains information on the endpoint.

On the other hand, data will be available in the near future only for lepton energies above 2.3 GeV. Thus we shall in the following also consider moments, in which the integration over n is restricted to a range $y_0 < y < 1 + \bar{\Lambda}/m_b$

$$\mathcal{M}_n(y_0) = \int_{y_0}^{1+\bar{\Lambda}/m_b} dy \, y^n \frac{d\Gamma}{dy}, \quad (17)$$

where realistic values for y_0 will be in the region of $y_0 = 0.9$. Introducing such a lower cut will change (16) to

$$\tilde{\mathcal{M}}_n^{(0)} = \Gamma_b \frac{2}{n+1} (1 - y_0^{n+1}), \quad (18)$$

from which we estimate that for $y_0 = 0.9$ the sixth moment will get about 52%, the tenth moment already about 70% contribution from the region $y_0 < y < 1$, at least in the naive parton model. On the other hand, an upper limit of n is given by the experimental resolution. If data on $b \rightarrow u$ semileptonic transitions is available only in the small window between 2.3 GeV and 2.6 GeV one may not expect enough data to extract moments higher than about ten. In what follows we shall thus concentrate on moments less than ten.

Next we turn to the nonperturbative corrections. They have been given in (3) to order $1/m_Q^2$. Taking the moments of (3) one obtains in the endpoint approximation (8)

$$\mathcal{M}_n = \tilde{\mathcal{M}}_n^{(0)} + \Gamma_b \left[\frac{\lambda_1}{3m_b^2} \left(\frac{10}{n+1} - 1 - n \right) + \frac{\lambda_2}{m_b^2} \left(\frac{22}{n+1} - 11 \right) \right]. \quad (19)$$

The dependence on n of the various terms in \mathcal{M}_n reflects, how singular the contribution is at the endpoint of the lepton spectrum. The most singular term is the one with the derivative of the δ function; this leads to a linear dependence in n . The terms behaving like a δ function yield constant terms in the moments, while terms with step functions will decrease as $1/n$ if n becomes large.

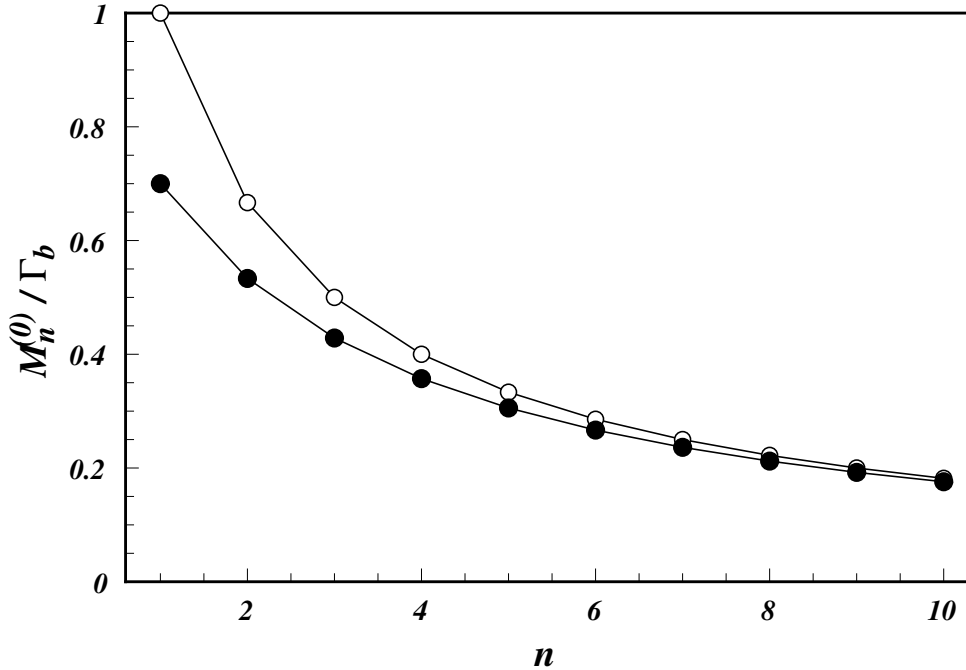


Figure 1: Comparison of the parton model moments for the full y dependence (full dots) versus the endpoint approximation (open circles).

In a similar way as for the parton model we may estimate the effects of a lower cut off y_0 according to (17). For the terms involving step function the result is qualitatively the same as for the parton model, while for the contributions with δ function like singularities there is no dependence on the lower cut, since these are concentrated at $y = 1$.

Higher moments will become more and more sensitive to what happens in the endpoint region. Thus (19) is not valid for n becoming too large. In order to estimate the value of n , where the expansion breaks down, we have to consider an even more singular contribution. This is contained in the next order of the $1/m_Q$ expansion, and has the form

$$\frac{d\Gamma}{dy} \sim \frac{a_3}{m_b^3} \delta''(1 - y), \quad (20)$$

where the parameter a_3 is related to the matrix element

$$\langle B(v) | \bar{h}_v(iD_\mu)(ivD)(iD^\mu)h_v | B(v) \rangle.$$

Taking the moment of this gives a contribution quadratic in n

$$M_n \sim \Gamma_b n(n-1) \frac{a_3}{m_b^3}. \quad (21)$$

Neglecting the higher orders in the $1/m_Q$ expansion of the moments is only justified, if

$$n(n-1) \frac{a_3}{m_b^3} < n \frac{\lambda_1}{m_b^2}.$$

Estimating a_3 to be $(|\lambda_1|)^{3/2} \sim (500 \text{ MeV})^3$ one obtains

$$n < \frac{m_b}{\sqrt{|\lambda_1|}} \sim 10, \quad (22)$$

which means that only the nonperturbative contributions to the first few moments may be calculated to lowest order in the $1/m_Q$ expansion. It is a fortunate circumstance that this upper limit in n coincides with the maximal n accessible in experiment.

In order to estimate higher moments one has to perform a resummation of the most singular terms at the endpoint to all orders in $1/m_Q$, in other words, one has to include these effects using the nonperturbative function $F(x)$ defined in (6). In terms of this the rate is given by (5), which describes the behavior of the lepton spectrum close to the endpoint, namely over a region of the order $1 - y \sim \sqrt{|\lambda_1|}/m_b$. There is, however, an even smaller region $1 - y \sim (\sqrt{|\lambda_1|}/m_b)^2$, the resonance region, in which only a few resonances contribute to the spectrum. This region will start to contribute significantly to the moments for

$$n \sim \left(\frac{m_b}{\sqrt{|\lambda_1|}} \right)^2 \sim 100 \quad (23)$$

which means that moments with $n > 100$ will be determined from the contributions of only very few light resonances.

The function F is genuinely nonperturbative and it has been considered using several models. One frequently used model is the one of Altarelli et al. [14], which has been rewritten in terms of the nonperturbative function $F(x)$ [20] given by

$$F(x) = \frac{\bar{\Lambda}}{\sqrt{\pi} p_F} \exp \left(-\frac{1}{4} \left(\frac{\bar{\Lambda} \rho}{p_F(1-x)} - \frac{p_F}{\bar{\Lambda}}(1-x) \right)^2 \right). \quad (24)$$

Here $\bar{\Lambda} = m_B - m_b$, where m_B is the mass of the B -meson. The second parameter p_F is the so called Fermi-momentum which corresponds to the motion of the heavy quark inside of the heavy meson; see [20] for precise definition. Finally, ρ is implicitly given in terms of the other two parameters by

$$\bar{\Lambda} = \frac{p_F \rho e^{(\rho/2)} K_1(\rho/2)}{\sqrt{\pi}}, \quad (25)$$

where K_1 is a modified Bessel function.

The model as given in [20] has only one parameter ρ , which has a physical interpretation, namely $\rho = m_{\text{Spectator}}^2/p_F^2$. One may also relate the model parameters to the QCD matrix element λ_1 , since appropriate moments of F are related to matrix elements of powers of covariant derivatives between heavy meson states. In this way one obtains the relation

$$1 - \frac{\lambda_1}{3\bar{\Lambda}^2} = \pi \frac{2 + \rho}{\rho^2 K_1^2(\rho/2)} e^{-\rho}, \quad (26)$$

which may be used to determine the value of the model parameter ρ in terms of $\bar{\Lambda}$ and λ_1 ; it has been pointed out in [20] that only the combination $\xi = -\lambda_1/(3\bar{\Lambda}^2)$ enters in the model. In particular, eq.(26) has no solution, if ξ is larger than 0.57. For a value of $\bar{\Lambda}$ of 500 MeV, this means that the model cannot accommodate a value for $-\lambda_1$ of more than 0.42 GeV^2 . For this value we have $\rho = 0$, and the nonperturbative function simplifies

$$F(x) = \frac{2}{\pi} \exp \left(-\frac{(1-x)^2}{\pi} \right). \quad (27)$$

We shall use this model to estimate the effects of the most singular terms occurring in higher orders in the $1/m_b$ expansion.

The value of λ_1 is not yet known accurately. We shall consider below a “small” value $\lambda_1 = 0.3 \text{ GeV}^2$ as well as the largest value possible in the above model, $\lambda_1 = 0.43 \text{ GeV}^2$. The first value of λ_1 corresponds to $\rho = 0.35$, while the large one is the limiting case $\rho = 0$. In our final result we shall also consider a “large” value $\lambda_1 = -0.6 \text{ GeV}^2$. Furthermore, we will use $m_b = 4.7 \text{ GeV}$ and $\bar{\Lambda} \sim 500 \text{ MeV}$ in the following numerical analysis.

In Fig.2 we plot the nonperturbative corrections $\delta\mathcal{M}_n^{(np)}$ to the moments, $\delta\mathcal{M}_n^{(np)} = \mathcal{M}_n^{(np)} - \tilde{\mathcal{M}}_n^{(0)}$. The upper plot corresponds to $\lambda_1 = -0.3 \text{ GeV}^2$, and the lower one to the maximal value for λ_1 which can be accommodated in the model (24), $\lambda_1 \sim -0.43 \text{ GeV}^2$. The solid dots are the nonperturbative corrections according to (19), while the solid triangles are the corrections using the model (24) for the nonperturbative function F .

We have also plotted separately the contributions to the moments originating from the term linear in n of (19) (open circles) and the rest, i.e. the constant terms and terms decreasing with n (open squares).

In both cases, small and large λ_1 , one finds a substantial contribution from the chromomagnetic moment term λ_2 at least for small moments. The term from the kinetic energy operator has a linear dependence on n (c.f. (19)) while the chromomagnetic term behaves like a constant for large n . The linear terms of (19) are well reproduced by the model for the nonperturbative function; this is to be expected, since the nonperturbative function contains only the most singular contribution in each order of the $1/m_b$ expansion, i.e. the leading twist term. On the other hand, from the fact that the linear term

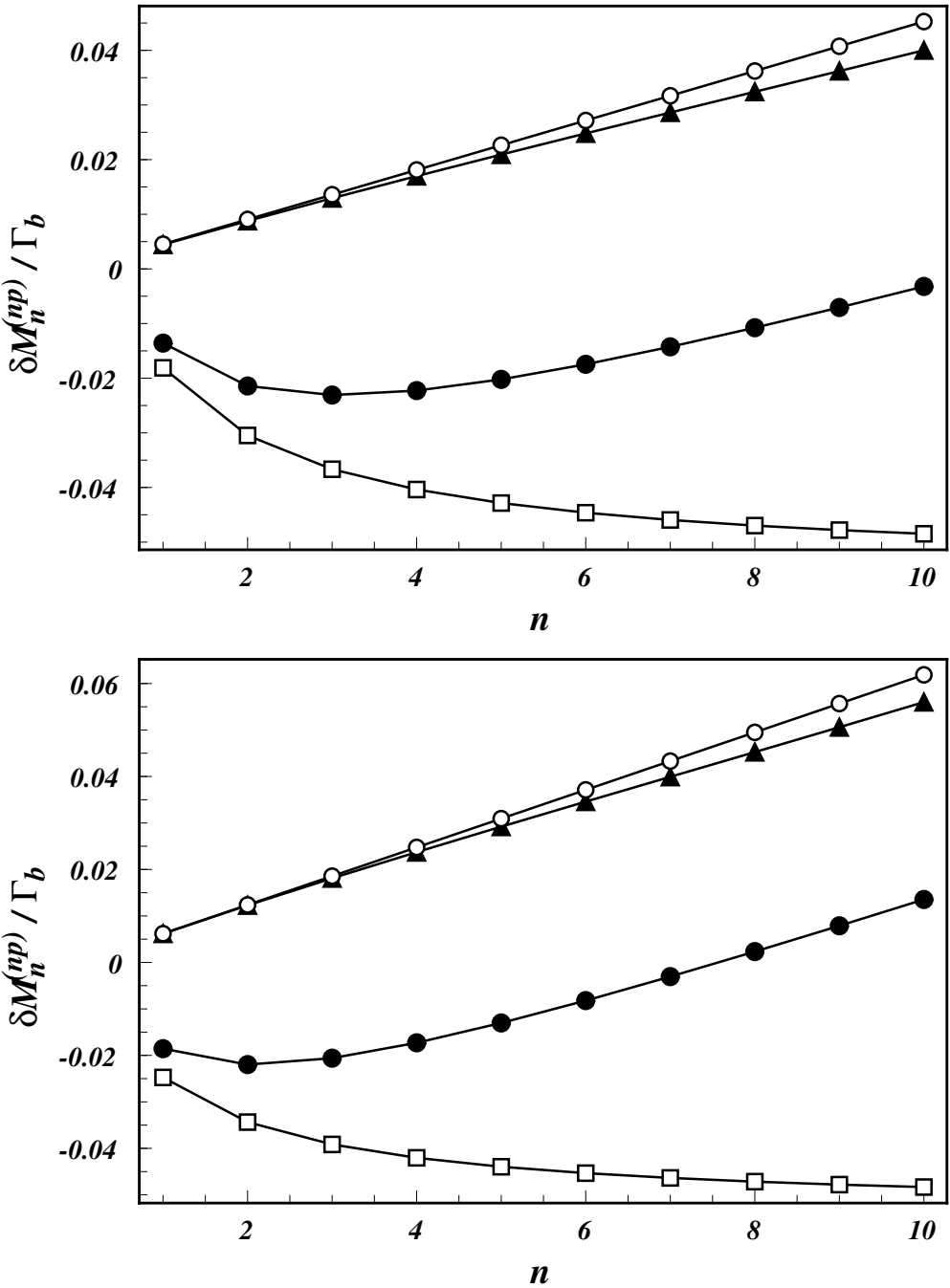


Figure 2: The nonperturbative corrections to the moments for $\lambda_1 = -0.3 \text{ GeV}^2$ (upper figure) and $\lambda_1 = -0.43 \text{ GeV}^2$ (lower figure). The solid dots are the corrections using the lowest nontrivial contributions (19), the solid triangles are the corrections from the nonperturbative function as given in (27), the open circles are the contributions from the $n\lambda_1$ alone in (19), and the open boxes are the contributions except the $n\lambda_1$ term.

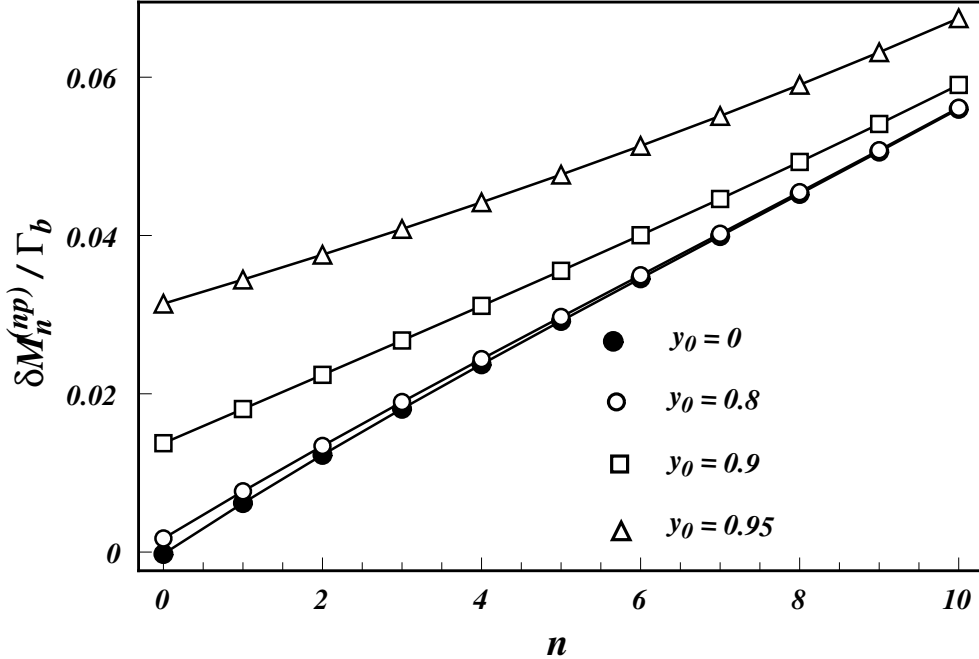


Figure 3: The nonperturbative corrections to the moments, including a lower cut of y_0 in the integration as in (17). We use $\rho = 0$, corresponding to $\lambda_1 = -0.43 \text{ GeV}^2$.

in n from (19) already approximates the nonperturbative function quite well, one may conclude that the expansion (19) is in fact sufficient for the range of n we are considering. In other words, the leading twist contribution modelled by the ansatz (24) may be replaced by the term proportional to λ_1/m_b^2 in the $1/m_b$ expansion of the moments with high accuracy.

However, the result (19) differs from what the nonperturbative function gives, mainly because of the chromomagnetic moment term and the constant terms proportional to λ_1 . These terms are less singular than the contribution of $n\lambda_1$, but they contribute substantially to the moments $n < 10$. On the other hand, the leading twist terms indicate that the $1/m_b$ expansion is satisfactory for $n < 10$ and we conclude the expansion (19) is justified for the moments in the range considered.

Finally, one may also consider the effect of a lower cut off y_0 in the integration over y as in (17). The strongest effects are expected for large λ_1 , so we plot in fig.3 the nonperturbative corrections for $\rho = 0$ in the model (24), for different values of the cut off y_0 . For the realistic case $y_0 = 0.9$ one finds only small corrections for $4 < n < 10$, and the conclusion concerning the minimal n obtained from the parton model remain valid.

Next we consider the radiative corrections. In Fig.4 we plot these correc-

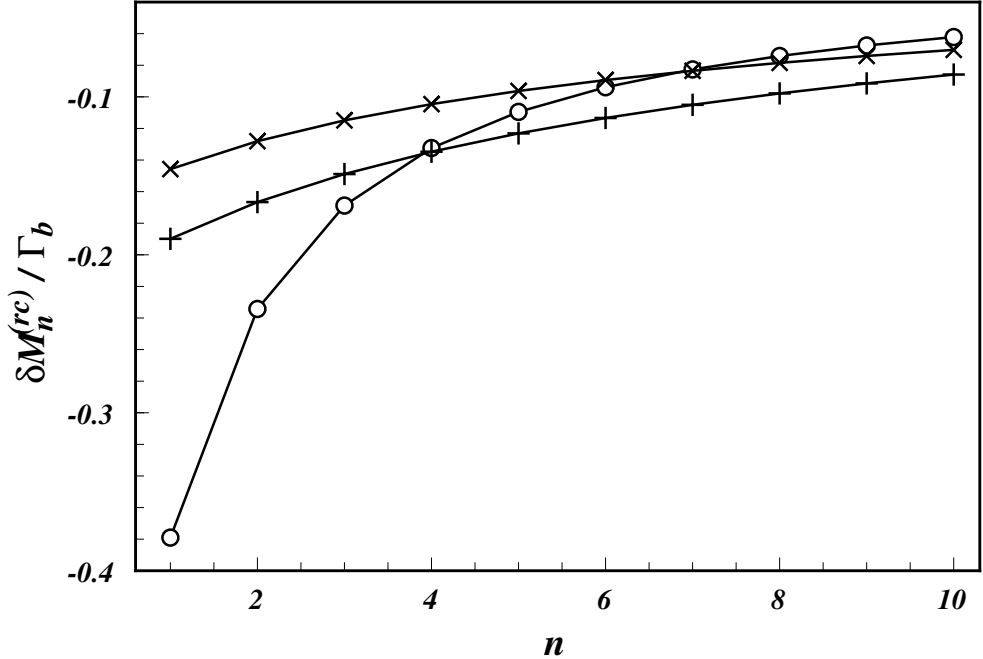


Figure 4: The radiative corrections to the moments. Open circles correspond to (7) with $\alpha_s(m_b) = 0.26$, the crosses correspond to (9) with $\alpha_s(m_b) = 0.26$, and the x'es are obtained from (11).

tions to the moments $\delta M_n^{(rc)}$ obtained from the one loop result (7), from the exponentiation of the leading double logarithms, for both fixed scale $\mu = m_b$ and for variable scale $\mu = m_b(1 - x)$. We use in (7) the value of α_s at m_b , $\alpha_s(m_b) = 0.26$, corresponding to $\Lambda_{QCD} = 250$ MeV.

The radiative correction contribution to the moments with $n > 4$ is rather stable, in other words, it does not depend on how one deals with the endpoint singularities. Compared to the nonperturbative corrections for small λ_1 they are much larger, dominating the corrections to the moments. This smallness of the nonperturbative corrections is due to an almost cancellation between the contributions of λ_1 and λ_2 in the region of n we are considering.

The effect of a lower cut in the y integration for the moments as in (17) leads to a doubly logarithmic dependence of the form $\ln^2(1 - y_0)$ on the lower cut y_0 , and, if y_0 comes close to 1, the effects of the lower cut may become large, forcing us to go to higher n . However, numerically it turns out that with realistic values of y_0 the situation still remains under control. This is shown quantitatively in fig.5, where we use expressions (7) (upper figure) and (9) (lower figure) to estimate the effect of a lower bound. Again, for the realistic value $y_0 = 0.9$ the corrections to the moments $4 < n < 10$ are less

n	$\Delta(n)$	$\sigma(n)$
0	2.000	-1.000
1	1.750	-0.750
2	1.574	-0.611
3	1.441	-0.521
4	1.335	-0.457
5	1.249	-0.408
6	1.176	-0.370
7	1.114	-0.340
8	1.060	-0.314
9	1.013	-0.293
10	0.971	-0.274

Table 1: Numerical values for the functions $\Delta(n)$ and $\sigma(n)$

than ten per cent.

Our main conclusion is thus that one may use the combined expansion for the moments below $n = 10$, which is given by

$$\begin{aligned} \mathcal{M}_n = & \Gamma_b \left[\frac{2}{n+1} + \frac{\lambda_1}{3m_b^2} \left(\frac{10}{n+1} - 1 - n \right) + \frac{\lambda_2}{m_b^2} \left(\frac{22}{n+1} - 11 \right) \right. \\ & \left. - \frac{4\alpha_s(m_b)}{3\pi(n+1)} \left(\frac{5}{4} + \pi^2 \right) - \frac{4\alpha_s(m_b)}{3\pi} \left(\Delta(n) + \frac{31}{6}\sigma(n) \right) \right] \\ & + \mathcal{O} \left(\left(\frac{\bar{\Lambda}}{m_b} \right)^3, \alpha_s^2(m_b), \left(\frac{\bar{\Lambda}}{m_b} \right)^2 \alpha_s(m_b) \right) \end{aligned} \quad (28)$$

where we have defined

$$\begin{aligned} \Delta(n) &= \sum_{k=0}^n \binom{n}{k} (-1)^k \left(\frac{1}{k+1} \right)^3 = \frac{1}{n+1} \left[\left(\sum_{k=1}^{n+1} \frac{1}{k} \right)^2 + \sum_{k=1}^{n+1} \frac{1}{k^2} \right] \\ &\longrightarrow \frac{1}{n} \ln^2 n \text{ for } n \gg 1 \\ \sigma(n) &= \sum_{k=0}^n \binom{n}{k} (-1)^{k+1} \left(\frac{1}{k+1} \right)^2 = -\frac{1}{n+1} \sum_{k=1}^{n+1} \frac{1}{k} \longrightarrow -\frac{1}{n} \ln n \text{ for } n \gg 1 \end{aligned} \quad (29)$$

The values for $\Delta(n)$ and $\sigma(n)$ are tabulated in tab.1.

Furthermore, the fact that data will be available only for $y > y_0 \sim 0.9$ only has a small effect on the moments in the range of n considered; the moments including a lower cut y_0 may still be treated in the combined expansion.

The final result for the moments is plotted in Fig.6, where the moments obtained from the combined expansion in $\alpha_s(m_b)$ and $\bar{\Lambda}/m_b$ according to (28)

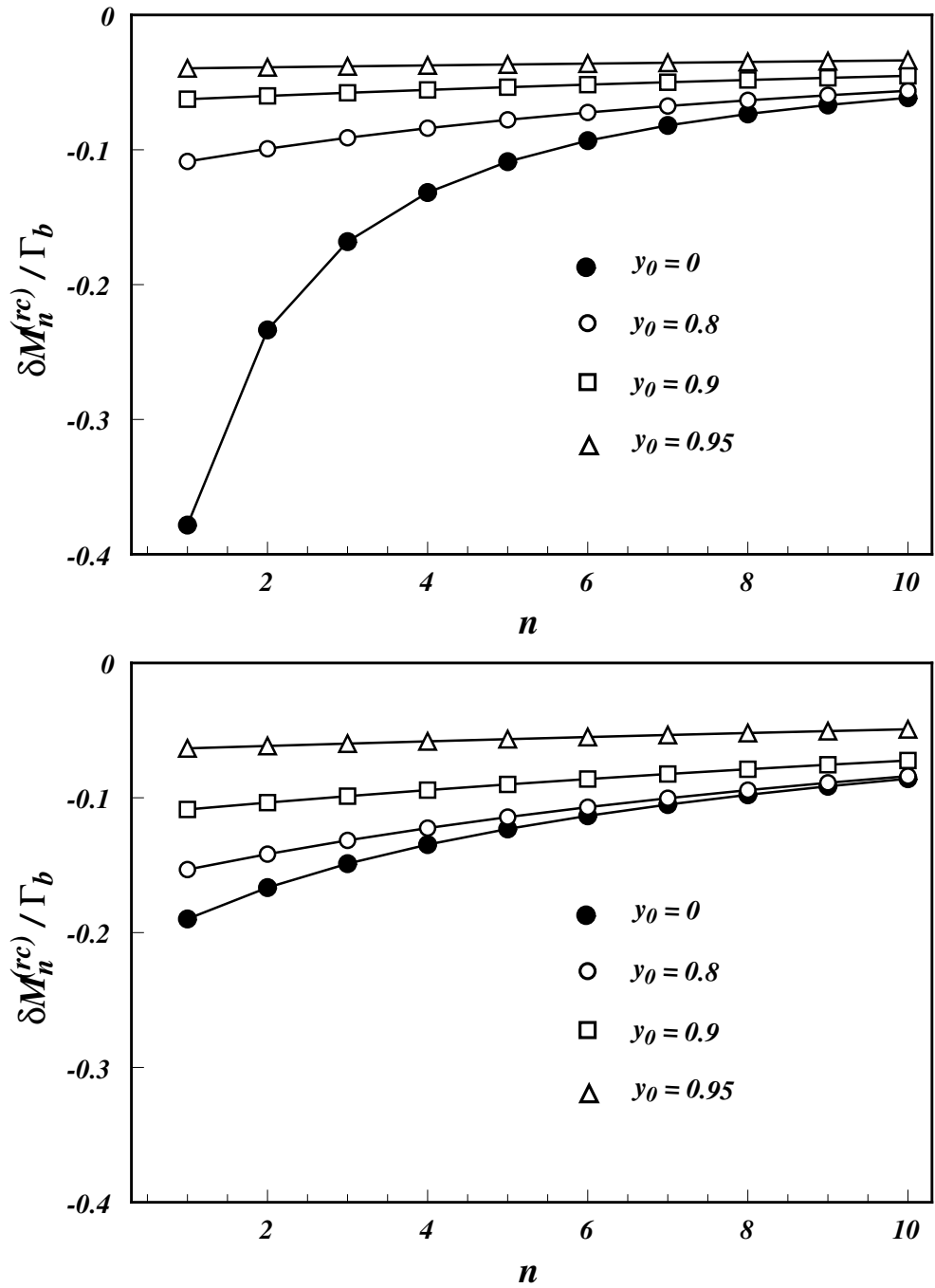


Figure 5: The effect of a lower cut off y_0 (c.f. (17)) on the radiative corrections to the moments. The upper figure are the moments obtained from (7) with lower cut off, while the lower plot is obtained from (9).

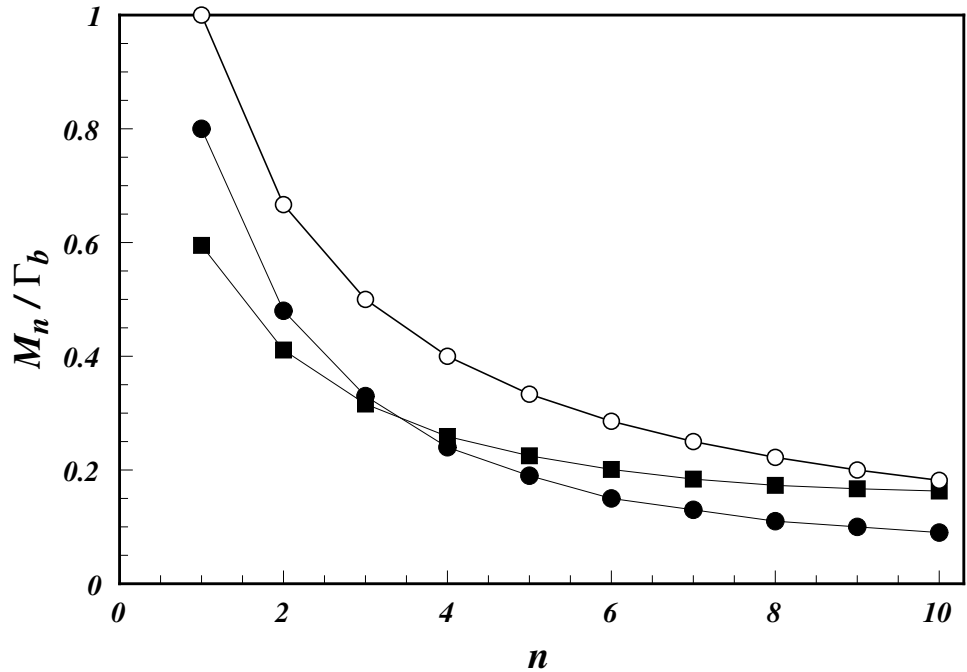


Figure 6: The final result for the moments, including both radiative and nonperturbative corrections according to (28). The solid dots are the result for $\lambda_1 = -0.3 \text{ GeV}^2$, the solid boxes are for $\lambda_1 = -0.6 \text{ GeV}^2$. For comparison we also plot the parton model result (open circles).

are shown. The solid dots are the result for “small” $\lambda_1 = -0.3 \text{ GeV}^2$, and the solid boxes are for “large” $\lambda_1 = -0.6 \text{ GeV}^2$.

To summarize, one may analyze the moments up to 12 before the corrections become too big, of order 100%. We also see that nonperturbative corrections are very small for small values of λ_1 , and key role is played by the radiative ones. The reason for the smallness of nonperturbative corrections is an almost complete cancellation between the terms proportional to λ_1 and λ_2 . For the case $\lambda_1 = -0.6 \text{ GeV}^2$ the cancellation is only partial and nonperturbative correction are sizable and positive. This indicates that higher twist effects may play an important role also in the endpoint region, and taking into account only the leading twist contribution, corresponding to the function F , is not enough. This remark, however, applies to a precise description of the spectrum in the endpoint region, while for the moments with sufficiently small n it is safe to use the combined expansion in $\alpha_s(m_b)$ and $\bar{\Lambda}/m_b$, which contains pieces of nonleading twist in the constant terms and the contributions decreasing with n .

4 Conclusions

Since data on $b \rightarrow u$ transitions will be restricted to a small window between 2.3 and 2.6 GeV, it is mainly the endpoint of the spectrum which will be accessible in experiment. On the other hand, the endpoint region is the most difficult region from the theoretical point of view, since here large radiative corrections are entangled with large nonperturbative effects. In fact, it is not even obvious, whether and how one may distinguish the two sources of corrections close to the endpoint.

The main result of this paper is that one may define suitable averages of the inclusive decay distribution of semileptonic $b \rightarrow u$ transitions, which on one hand may be calculated reliably, and which on the other hand are mainly sensitive in the window between the kinematic endpoints of $b \rightarrow c$ and $b \rightarrow u$ semileptonic decays. We have concentrated on moments of the energy spectrum of the charged lepton and have performed a detailed numerical analysis, which shows that moments for $n < 10$ may be systematically calculated in a combined $\alpha_s(m_b)$ and Λ/m_b expansion; both types of corrections may be studied systematically. Furthermore, the moments with $n > 4$ are sensitive mainly in the experimentally accessible window. Thus there is indeed a region $4 < n < 10$ for which the moments defined above may be useful to perform a determination of $|V_{ub}|$.

In fact, such a combined expansion is even valid for moments defined with a lower cut off y_0 , as given in (17) as long as y_0 is not too close to one. Furthermore, for a realistic value $y_0 = 0.9$ the deviations of the moments including a cut from the full ones are small in the region of n considered. Thus for an experimental analysis one may as well deal with the moments including a cut.

In order to extract $|V_{ub}|$ from these moments one has to know the two matrix elements λ_1 and λ_2 . While λ_2 is known from the hadron spectrum, λ_1 is still uncertain; we have used typical “large” and “small” values, but one may hope to extract this parameter from experiment eventually.

One possibility to perform a determination of λ_1 is in fact to use the moments defined above. The ratio of two moments will depend only on λ_1/m_b^2 , λ_2/m_b^2 and $\alpha_s(m_b)$. The strong coupling and λ_2 are known, and one may in principle extract λ_1 and m_b from two ratios of moments. After having done this one may then use any one of the moments to obtain Γ_b and hence $|V_{ub}|$. To proceed along these lines one needs a measurement of three moments in the range $4 < n < 10$; any measurement of additional moments may be used to cross check the n dependence of the moments.

The idea presented here may be refined in various aspects, and we consider this paper as a first try to study whether one may extract $|V_{ub}|$ using the moments of the decay distributions. As far as the radiative corrections are concerned, we have only considered the singular and nonvanishing terms

close to the endpoint. In this point one may refine the analysis by taking into account the complete corrections, which may be found in the literature. Furthermore, also the corrections of order $\bar{\Lambda}/m_b$ have been considered [21] and may be also included in the analysis. However, we do not expect that any of these higher order corrections will change any of our conclusions.

Finally, one may also think of considering other averages of decay distributions and generalize the moments according to

$$\widetilde{\mathcal{M}}_n = \int_0^{1+\bar{\Lambda}/m_b} dy \mathcal{F}_n(y) \frac{d\Gamma}{dy} \quad (31)$$

where \mathcal{F}_n is some set of functions. A good choice of \mathcal{F}_n may possibly allow a more reliable calculation of the corresponding moments $\widetilde{\mathcal{M}}_n$, and on the other hand be more sensitive to the experimentally accessible region.

Acknowledgements

We want to thank the theory group of SLAC and especially M. Peskin and S. Brodsky for the hospitality extended to both of us. It was a pleasure to discuss issues concerning this paper with S. Brodsky, M. Peskin and H. Anlauf. B.B. wants to thank M. Shifman and T.M. wants to thank D. Cassel, M. Neubert and N. Uraltsev for discussions.

References

- [1] J. Chay, H. Georgi, B. Grinstein, Phys. Lett. **B247** (1990) 399.
- [2] I. Bigi, N. Uraltsev, A. Vainshtein Phys. Lett. **B293** (1992) 430.
- [3] B. Blok and M. Shifman, Nucl. Phys. **B399** (1993) 441, 459.
- [4] I. Bigi, B. Blok, M. Shifman, N. Uraltsev, A. Vainshtein, The Fermilab Meeting Proc. of the 1992 DPF meeting of APS, C.H. Albright et al., Eds. World Scientific, Singapore 1993, vol.1, p. 610.
- [5] I. Bigi, M. Shifman, N. Uraltsev and A. Vainshtein, Phys. Rev. Lett. **71** (1993) 496.
- [6] B. Blok, L. Koyrakh, M. Shifman, A. Vainshtein, Phys. Rev. **D49** (1994) 3356.
- [7] A. Manohar and M. Wise, Phys. Rev. **D49** (1994) 1310.
- [8] T. Mannel, Nucl. Phys. **B413** (1994) 396.

- [9] M. Neubert, preprint CERN-TH.7113/93.
- [10] I. Bigi et al, preprint CERN-TH.7129/94.
- [11] T. Mannel and M. Neubert , preprint CERN-TH.7156/94.
- [12] A. Ali and E. Pietarinen, Nucl. Phys. **B154** (1979) 519.
- [13] N. Cabibbo, G. Corbo and L. Maiani, Nucl. Phys. **B155** (1979) 83.
- [14] G. Altarelli et al., Nucl. Phys. **B208** (1982) 365.
- [15] G. Corbo, Nucl. Phys. **B212** (1983) 99.
- [16] M. Jezabek and J. H. Kühn, Nucl. Phys. **B320** (1989) 20.
- [17] A. Falk, A. Manohar, E. Jenkins, M. Wise, Phys. Rev. **D49** (1994) 3367.
- [18] M. Neubert, Phys. Rev. **D46** (1992) 1076.
- [19] P. Ball and V.M. Braun, Phys. Rev. **D49** (1994) 2472.
- [20] I. Bigi et al, preprint CERN-TH.7159/94.
- [21] A specific $1/m_b^3$ contribution has been considered in I. Bigi and N. Uraltsev, CERN Report CERN-TH.7020/93.